Chapter 3. Hamilton's principle

N°	Title	Level	P.	Features
3.1	The Lorentz force	⋆⋆	116	Hamilton's principle applied to an electromagnetic problem
3.2	Relativistic particle in a central force field	⋆⋆⋆	117	Relativistic Binet's equation
3.3	Principle of least action?	⋆⋆⋆	118	Justification of the concept of "least action"
3.4	Minimum or maximum action?	⋆⋆	119	Why the action is not always minimal
3.5	Is there only one solution which makes the action stationary?	⋆⋆	120	Hamilton's principle. Through two points may pass several trajectories
3.6	The principle of Maupertuis	⋆⋆	121	Alternative to the Hamilton principle for the determination of the trajectories
3.7	Fermat's principle	⋆⋆	122	Hamilton's principle in the domain of optics
3.8	The skier strategy	⋆⋆⋆	122	Calculus of variations for the brachistochrone
3.9	Free motion on an ellipsoid	⋆⋆	123	Calculus of variations with a holonomic constraint. Lagrange multipliers
3.10	Minimum area for a fixed volume	⋆⋆	124	Calculus of variations with an integral constraint. Lagrange multipliers
3.11	The form of soap films	⋆⋆⋆	125	Amusing application of Hamilton's principle. Calculus of variations
3.12	Laplace's law for surface tension	⋆⋆⋆	127	Hamilton's principle applied to hydrostatics
3.13	Chain of pendulums	⋆⋆	128	Hamilton's principle for a continuous system
3.14	Wave equation for a flexible blade	⋆⋆	128	Building a Lagrangian density
3.15	Precession of Mercury's orbit	⋆⋆⋆	128	Hamilton's principle in the context general relativity

One chooses a system of perpendicular axes in the inclined plane: horizontal XX', and YY' along the direction of steepest upward slope. The center O of the axle is characterized by its coordinates X et Y in this frame with an arbitrary origin A. The direction $C'C$ makes an angle θ with the horizontal line XX'. We denote by ϕ and ϕ' the angles which mark the positions of reference points on the circumference of the wheels with respect to the line normal to the inclined plane. Thus, the system is described in terms of 5 generalized coordinates $(X, Y, \theta, \phi, \phi')$.

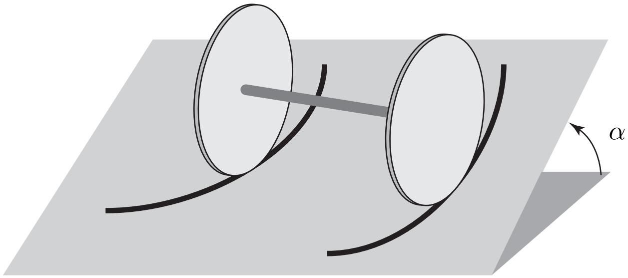

Figure 1.4 – Axle with independent wheels rolling without slipping on a inclined plane.

1. There exist four scalar relationships concerning the constraints of rolling without slipping for each of the wheels (two per wheel). In fact, two of them are identical. Give the three independent constraint relationships and show that one of them is holonomic whereas the other two are not.

2. Introducing 3 Lagrange multipliers λ_1, λ_2, λ_3, write the 5 constrained Lagrange equations.

3. Interpret the 3 Lagrange multipliers in terms of contact forces.

4. To solve the 8 equations (5 Lagrange equations plus 3 constraint equations), it is judicious to change variables by defining $\sigma = (\phi + \phi')/2$ and $\delta = (\phi - \phi')$.

   Rewrite the Lagrange equations in terms of these new variables. According to the initial conditions, study the various types of behavior for the axle. In particular, give the equations of the motion if, initially, the axle center is located at A and sets off down the slope with a speed V_0, the axle itself being horizontal and having an initial angular velocity $\dot{\theta}(0) = \omega$.

5. In this framework, calculate the Lagrange multipliers λ_i which represent the reaction forces.

and the Lagrangian (difference between the kinetic and potential energies) is:

$$L = \frac{1}{2}m(\dot{x}^2 + \dot{y}^2 + \dot{z}^2) + q_e[\frac{1}{4}k(x^2 + y^2 - 2z^2) + \frac{1}{2}B(\dot{y}x - \dot{x}y)].$$

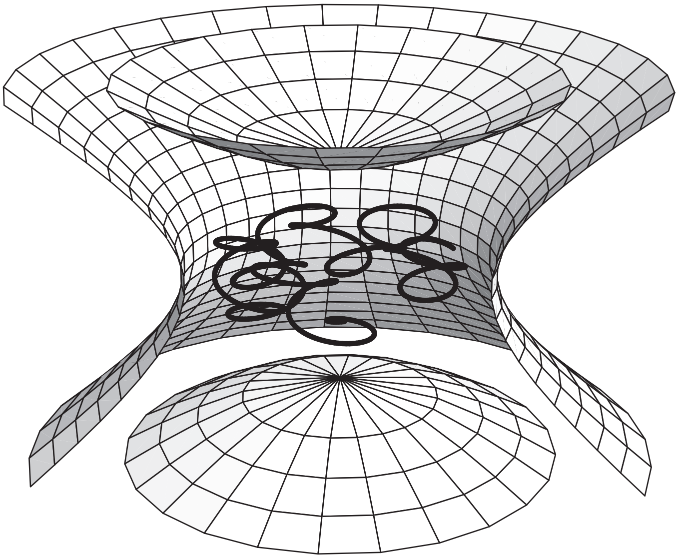

Figure 2.10 – Equipotential surfaces for the scalar potential employed in a Penning trap. A trajectory for the particle confined inside the trap is also shown in the figure.

2. Applying (2.4), Lagrange's equations can be derived as:

$$\begin{aligned} m\ddot{x} &= q_e(B\dot{y} + \frac{1}{2}kx); \\ m\ddot{y} &= q_e(-B\dot{x} + \frac{1}{2}ky); \\ m\ddot{z} &= -q_e kz \end{aligned}$$

The equation for the z variable can be written $\ddot{z} + \omega_a^2 z = 0$, with the axial angular frequency ω_a given in the statement. This equation is integrated at once to give:

$$z(t) = a\ \cos(\omega_a t + \phi).$$

It reflects a sinusoidal behaviour.

3.12. LAPLACE'S LAW FOR SURFACE TENSION [SOLUTION P. 158] ⋆ ⋆ ⋆

The Hamilton principle applied to hydrostatics.

Let us consider an incompressible liquid (mass density ρ) lying, under the influence of a vertical constant gravitational field g directed downwards, in a parallelepipedic channel along an infinite horizontal axis $y'y$ (to avoid the boundary effect in that direction). Let O be an arbitrary origin on $y'y$, and Ox a horizontal axis perpendicular to Oy; the upward vertical is Oz. The xOz plane is thus a section plane and the form of the surface is a curve $z(x)$. This form is determined, in a static way, by a minimization of the gravitational potential energy and the surface potential energy TS. The surface tension of the liquid in contact with the air is T, supposed to be constant, and S the air-liquid interface area. Because of the translational invariance along the $y'y$ direction, we can reason using a slice with unit thickness in that direction. The edges of the channel are taken at the abscissas $x = 0$ and $x = l$.

The liquid-air-wall interface points are assumed to be fixed at $z(0) = h = z(l)$. We wish to minimize the total potential energy with fixed bounds. Moreover, we have in addition the constraint of a constant volume.

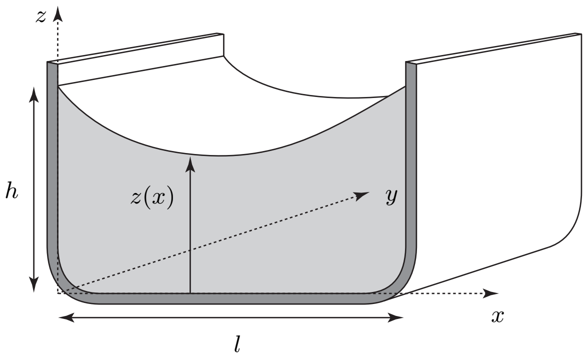

Figure 3.3 – Channel containing an incompressible liquid. In a slice of liquid, one defines a system of axes xOz. The form of the meniscus is given by the curve $z(x)$.

1. Give the expression of the functional of the total potential energy $V_P(z)$.
2. Express in the same way the functional of the volume $V(z)$.
3. Give the Euler-Lagrange equation constrained by a given volume, which allows the determination of the curve $z(x)$. It is useful to introduce the curvature radius $R(x)$ at each point.

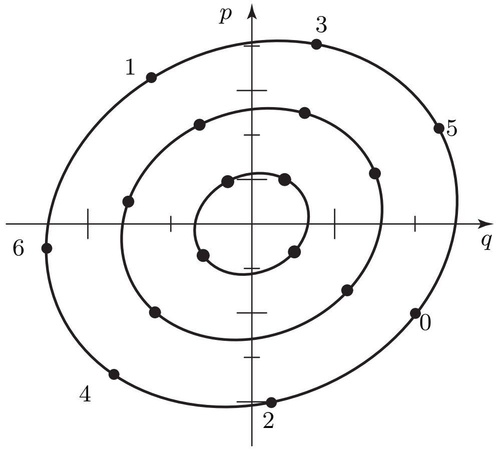

Figure 4.1 – Figure, in phase space, obtained from the positions of a system after periodic impulses labelled by the progressive numbers. This is the case of complex eigenvalues with unit modulus for the propagator.

- If the eigenvalues of the propagator are real or, equivalently, if the absolute values of the trace are larger than 2, the successive points lie on a hyperbola. Starting from a point located exactly on one of the asymptotes, the next point will lie closer to the fixed point according to a geometric progression. This is the convergent direction of the hyperbolic point. In contrast, starting from the other asymptote, the point will move away from the fixed point according to the inverse common ratio. A non singular initial deviation always leads to a departure from the fixed point. We say that we are faced with a **parametric resonance**. The fixed point is unstable. We have plotted such a situation in figure 4.2. We may remark that the stroboscopic order jumps from one branch to the other. This is a consequence of negative eigenvalues.

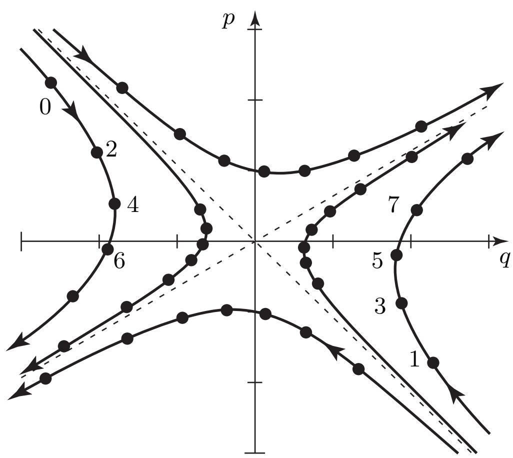

Figure 4.2 – Same situation as depicted in figure 4.1 in the case of a propagator having negative real eigenvalues.

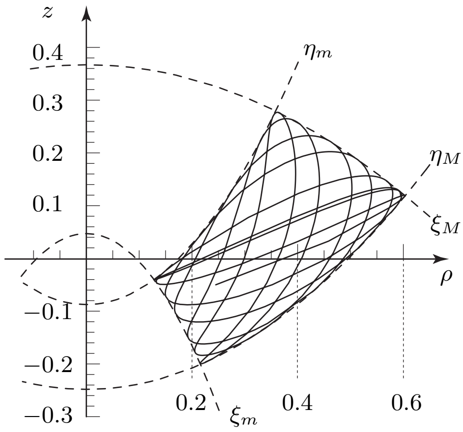

Figure 5.7 – Trajectory, in the plane (ρ, z), for a particle subjected to an attractive central electrostatic potential and a constant electric field along Oz.

5.10. ORBITS OF EARTH'S SATELLITES [STATEMENT AND FIGURES P. 248]

1. Let us begin with the obvious equality $|\boldsymbol{r} - \sigma\hat{z}|^2 = (\boldsymbol{r} - \sigma\hat{z})^2 = r^2 + \sigma^2 - 2\sigma r u$, where $u = \cos(\hat{r}, \hat{z})$ is the cosine between the radius vector and the Oz axis. It follows that

$$\frac{1}{|\boldsymbol{r} - \sigma\hat{z}|} = \frac{1}{r}\left(1 - \frac{2\sigma u}{r} + \frac{\sigma^2}{r^2}\right)^{-1/2}.$$

One works at a distance much larger than the distance between the two centers $\sigma/r << 1$; it is therefore justified to perform a truncated expansion of the square root, which relies on the well known formula $(1+\varepsilon)^{-1/2} = 1 - \varepsilon/2 + 3\varepsilon^2/8$. We arrive at the desired formula:

$$\frac{1}{|\boldsymbol{r} - \sigma\hat{z}|} = \frac{1}{r} + \frac{\sigma u}{r^2} + \frac{(3u^2 - 1)\sigma^2}{2r^3} + O(\sigma^3/r^4).$$

The expression for $1/|\boldsymbol{r} + \sigma\hat{z}|$ follows simply by changing σ into $-\sigma$.

The potential is deduced at once

$$V = -K\left[\frac{1}{r} + \frac{(3u^2 - 1)\sigma^2}{2r^3}\right].$$

This expression should be compared with the analog obtained from a revolution ellipsoid:

$$V = -GmM\left[\frac{1}{r} + \frac{(3u^2 - 1)(I - I_3)}{2Mr^3}\right].$$

5. Let us start from the Kepler trajectory given by

$$\frac{1}{Q} = \frac{1}{p}\left[1 + e\cos\alpha\right]$$

with $p = p_\alpha^2/(mK)$, $e = \sqrt{1 + 2E_c p_\alpha^2/(mK^2)}$. We make the substitutions of question 3 to find the equation of the trajectory for the harmonic oscillator:

$$\frac{l}{\rho^2} = \frac{1}{p} + \frac{1}{p}e\ \cos(2\phi).$$

Using the property $\cos(2\phi) = \cos^2\phi - \sin^2\phi$ and the Cartesian coordinates $x = \rho\cos\phi$, $y = \rho\sin\phi$, we arrive at the following equation:

$$\frac{x^2}{[pl/(1+e)]} + \frac{y^2}{[pl/(1-e)]} = 1.$$

This is the equation of an ellipse with its center at the origin, i.e., at the center of force, with a semi-minor axis $b = \sqrt{pl/(1+e)}$, and semi-major axis $a = \sqrt{pl/(1-e)}$. We present in figure 6.7, the correspondence between the two types of trajectories.

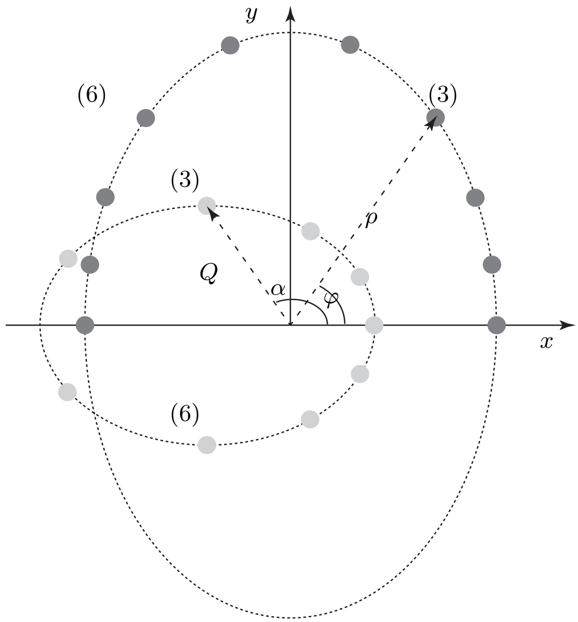

Figure 6.7 – Passage from the Kepler trajectory (in light grey) to the harmonic oscillator trajectory (dark grey) using the proposed contact transformation. The corresponding positions are displayed as full circles. A complete revolution around the Kepler ellipse corresponds to half a revolution on the harmonic oscillator ellipse.

This transformation allows us to generalize the notion of drift for the cyclotron orbit (we already met with such a drift by the addition of an electric field in problem 2.9). Let us imagine a supplementary force $\boldsymbol{F}$ acting on the particle. For simplicity we assume that this force arises from a potential $V(y)$, which depends on the y coordinate only and which varies slowly over a range of order of the cyclotron radius.

7. Write down the complete Hamiltonian, as well as the Hamilton equations relative to the (Y, P_Y) variables. Deduce that, on average over one revolution, the center of the cyclotron circle drifts along the Ox axis with a velocity to be determined.

This result is quite general: there is a drift perpendicular to the force, that is along the equipotential lines, with a velocity $\boldsymbol{V}_d = (\boldsymbol{B} \times \boldsymbol{F})/(q_e B^2)$.

7.8. ILLUMINATIONS CONCERNING THE AURORA BOREALIS [SOLUTION AND FIGURE P. 379] ⋆ ⋆

A fascinating natural phenomenon studied in detail. It is strongly advised to solve problems 2.9 and 7.7 before continuing.

To a good approximation, the Earth's magnetism is that of a magnetic dipole. In the magnetic equatorial plane, the magnetic field, which is perpendicular to it, takes the values $B_e = 0.31\,10^{-4}(R_T/R)^3$ Tesla (B_e is the value of B at the equator). In this formula R_T designates the Earth's radius and R the distance to the center of the Earth, for which the field is measured.

An electron of mass m, charge q_e and energy E crosses the equatorial plane, at a distance R from the center of the Earth, its velocity making an angle α with the direction of the magnetic field.

1. Recall the expression of the cyclotron frequency and show that the cyclotron radius (projection of the trajectory onto the equatorial plane) in the non-relativistic limit is:

$$R_c = \frac{\sqrt{2mE\sin^2\alpha}}{q_e B_e}.$$

In units of the Earth's radius, what is the value of this radius for $\alpha = \pi/4$ and for an energy $E = 60$ keV, at a distance $1.5R_T$ from the Earth's center. Give also the period of this cyclotron rotation.

Data: $q_e = 1.6\,10^{-19}$ C, $m = 9.11\,10^{-31}$ kg, $R_T = 6367$ km.

As we saw in problem 7.7, this force leads to a drift of the cyclotron motion with a velocity

$$\boldsymbol{V}_d = \frac{\boldsymbol{F}}{q_e B_e} \times \boldsymbol{N},$$

where $\boldsymbol{N} = \boldsymbol{B}/B$ is the unit vector along the field line. $\boldsymbol{N}$ is oriented in the south-north direction; $\boldsymbol{F}$ being radial, the drift velocity $\boldsymbol{V}_d$ is directed in the east-west or west-east direction, depending upon the sign of q_e. Finally the modulus of this drift velocity is simply $F/(q_e B_e)$ that is

$$V_d(R) = \frac{3E \sin^2 \alpha}{q_e B_e R}.$$

We show in figure 7.7 a number of trajectories for an electron in the Earth's magnetic field.

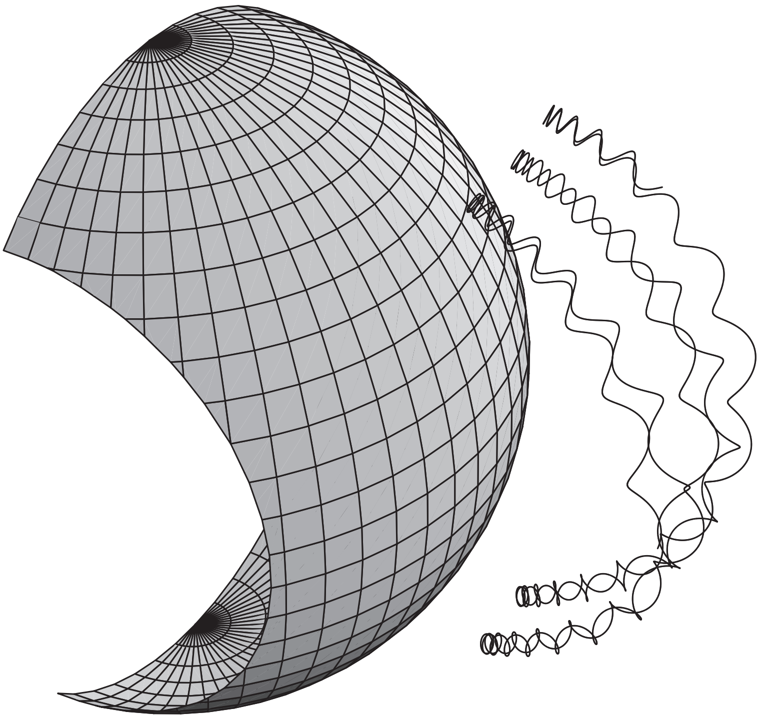

Figure 7.7 – Trajectories, in the Earth's magnetic field, calculated numerically using Hamilton's equations, for a 100 keV electron, passing at $1.6R_T$ at the magnetic equator, and making an angle 45 deg with the magnetic field. To clarify the various motions, we have chosen a magnetism much weaker than the real one.

We will see how to describe the behaviour of this system, by introducing the **Poincaré sections** and the basic notions for the **chaos phenomenon** will be presented and illustrated with the help of this experiment.

8.2. The model of the kicked rotor

The simplest mechanical system which exhibits a chaotic behaviour is the periodically kicked rotor. It is specified by an angle θ. When free, its Hamiltonian is given by $H_0(p) = p^2/(2I)$, in which I is the moment of inertia and the momentum $p = I\dot{\theta}$ is also the angular momentum. This Hamiltonian is a first integral. The phase space is a cylinder (θ is an angle which varies between 0 and 2π, whereas p can be any real number), and the trajectories are circles (transformed into straight lines if the cylinder is developed), since $p = \text{const}$.

Now we submit the rotor to a periodic impulse (period T and angular frequency $\omega = 2\pi/T$) which, without modification of the angle, instantaneously changes its momentum by a quantity proportional to $\sin\theta$. Without loss of generality, the period can be chosen as the unit time and the moment of inertia can be chosen as unity ($I = 1$, $T = 1$, $\omega = 2\pi$). The periodic impulse leads to an instantaneous variation of momentum $\Delta p = K \sin\theta_n$ for the nth kick.

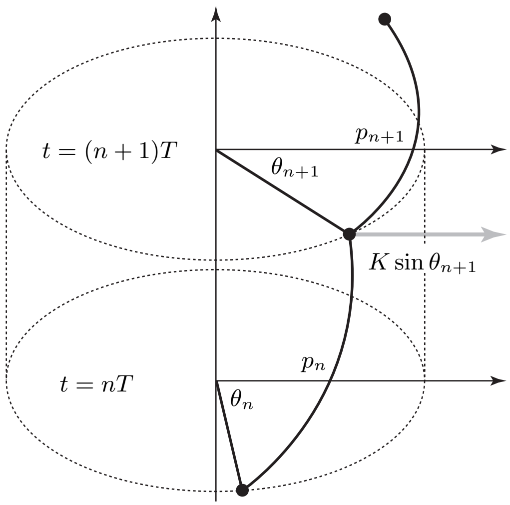

Figure 8.1 – Phase space for the kicked rotor. The cylinder represents the angle along the basic circle with the time along the generatrix. The grey arrow represents the periodic impulse which changes the angular velocity by a quantity proportional to the sine of the angle.

This Hamiltonian system is one-dimensional but it is non-autonomous and non-integrable; however it is simple to solve because, between each of the kicks, the angular velocity remains constant and between the impulses n and

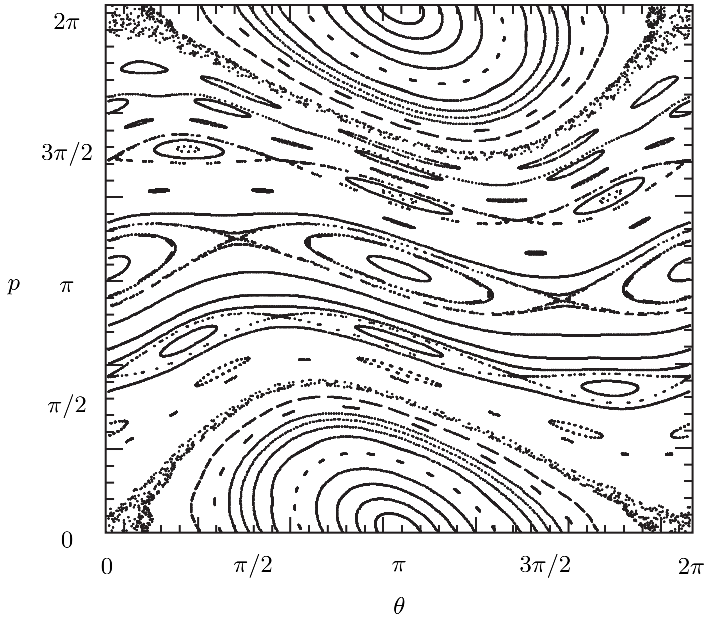

Figure 8.3 – Poincaré's section for the standard mapping with $K = 0.75$. The 36 initial conditions have been iterated 2000 times each.

At the limit of a null perturbation, they become straight lines; they are the remnants of the non-resonant tori discussed previously. The most clearly visible are located on either side of the value $p = \pi$. For other initial conditions, the filling in can take more time.

We also observe between these KAM curves the presence of "islets" formed by closed curves with elliptic shapes and, on each side of these islets, zones where the points seem to be scattered at random. These structures are the remnants of the resonant tori described above.

Thus, from the straight lines of the Poincaré sections without perturbation, there remain regular curves separated by zones with more complicated structure.

All these observations are the conclusion of the famous **KAM theorem** which can be stated as follows.

Let us consider an integrable (non degenerate) system. If one adds a weak perturbation, most of the invariant non-resonant tori do not disappear. These tori, filled in a dense way by the trajectories (a single one is sufficient), form the majority in the sense that the measure of the complement of their union is small for a weak perturbation.

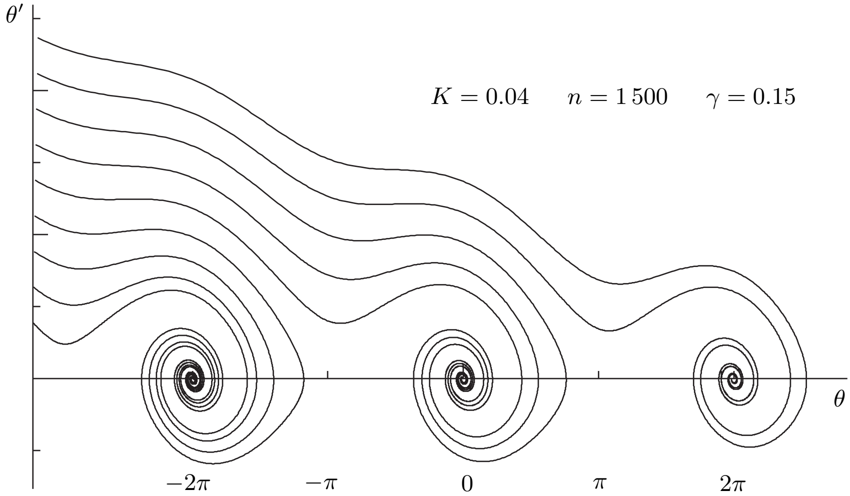

Figure 8.16 – Poincaré section corresponding to the damped pendulum, starting from 9 different initial conditions. The various parameters are indicated in the figure.

6. The Poincaré section corresponding to the damped pendulum is represented in figure 8.16 for a number of iterations equal to 1500, with the parameters $K = 0.04$ and $\gamma = 0.15$, and for 9 different initial conditions.

8.11. Stability of periodic orbits on a billiard table [statement and figure p. 409]

1. We choose an origin O and a point A on the cush which is specified by its curvilinear abscissa $s = \overset{\frown}{OA}$. At point A is defined the unit vector along the tangent $\boldsymbol{t}(s)$, oriented in the sense of increasing s, the unit vector along the normal $\boldsymbol{n}(s)$, oriented towards the interior of the table, and the unit vector perpendicular to the plane of the table $\boldsymbol{z}$, such that the trihedron $(\boldsymbol{t}, \boldsymbol{n}, \boldsymbol{z})$ is direct.

   Let B be a point close to A, such that $ds = \overset{\frown}{AB}$, where the tangent is $\boldsymbol{t}'$ and the normal $\boldsymbol{n}'$. The directions along $\boldsymbol{n}$ and $\boldsymbol{n}'$ intersect at a point C. The circle of center C and radius $R = CA$ is called the osculatory circle, and R is the radius of curvature at the point A. The convention is such that

$$d\boldsymbol{t} = \boldsymbol{t}' - \boldsymbol{t} = \frac{ds}{R}\,\boldsymbol{n} = \frac{ds}{R}\,(\boldsymbol{z} \times \boldsymbol{t}).$$

   With such a definition, the radius of curvature is positive, $R > 0$, if concavity is directed inward, and negative, $R < 0$, if it is directed outward.